Available online at www.eccomasproceedia.org
Eccomas Proceedia COMPDYN (2017) 2227-2238

ECCOMAS
Proceedia

COMPDYN 2017
6th ECCOMAS Thematic Conference on
Computational Methods in Structural Dynamics and Earthquake Engineering
M. Papadrakakis, M. Fragiadakis (eds.)
Rhodes Island, Greece, 15–17 June, 2017

THRUST NETWORK ANALYSIS OF MASONRY VAULTS SUBJECT TO VERTICAL AND HORIZONTAL LOADS

Francesco Marmo[1], **Daniele Masi**[1], **Salvatore Sessa**[1], **Ferdinando Toraldo**[1] **and Luciano Rosati**[1]

[1] Department of Structures for Engineering and Architecture
University of Naples Federico II
e-mail: f.marmo@unina.it

Keywords: Masonry, Arch, Vault, Limit thickness, Load bearing capacity.

Abstract. *We illustrate the assumptions underlying a recent reformulation of the Thrust Network Analysis (TNA), a methodology that allows one to model internal forces within masonry arches and vaults by means of a network of thrusts. The proposed version of the TNA allows for analysis of structures of complex geometry, with openings or free edges, subjected to the combined action of vertical and horizontal loadings. A series of numerical examples are reported to show how the method can be applied to evaluate the limit geometric proportions, e.g., minimum thickness, or the horizontal load bearing capacity of masonry arches and vaults.*

Peer-review under responsibility of the organizing committee of COMPDYN 2017.
doi: 10.7712/120117.5562.17018

1 INTRODUCTION

Stresses in masonry arches or vaults at failure are usually considerably lower than those required to cause material failure; hence stability of such kind of structures is basically due to their shape and self-weight magnitude and distribution [6]. This peculiarity has been an advantage prior to the development of structural analysis since stability of a full scale structure could be assessed on a scale model: the real structure was erected by scaling up the dimensions of a prototype or an existing structure while keeping constant the relative proportions [7].

One of the first rational approaches to the stability of masonry arches was found in the analogy between the shape of masonry arches in equilibrium and that of hanging cables in tension. Such an analogy (or catenary principle) is known since the 17th century and was first presented by Robert Hooke [8] in a famous anagram; the analogy was ultimately motivated by Heyman thanks to the limit analysis principles [5].

The Thrust Network Analysis (TNA) is a methodology based on Heyman's principles and is used for modeling stresses in masonry vaults as a discrete network of forces in equilibrium with gravitational loads. It was recently contributed by O'Dwyer [10] and fully developed by Block and coworkers in recent times [2, 3]. Alternative approaches can be found in [1, 4, 11].

Reducing the bias by the quoted authors in favor of a graphical interpretation of the method, Block's version of the TNA has been recently reformulated by discarding the dual grid and focusing only on the primal grid, thus significantly enhancing the computational performances of the method [9]. Such a reformulation of the TNA also includes horizontal forces in the analysis as well as holes or free edges in the vault. The coefficient matrices entering the solution scheme have been obtained by assembling the separate contribution of each branch, thus avoiding the ad-hoc node numbering and branch orientation required by Block's approach.

Numerical examples, regarding the application of the method to the evaluation of limit thickness or horizontal bearing capacity of some vaulted structures are illustrated to show the effectiveness and robustness of the TNA in assessing the safety conditions of existing masonry vaults.

2 Thrust network analysis

Equilibrium of vaulted structures can be studied by considering a network of thrusts, i.e. compressive forces acting within the structure in equilibrium with the applied loads. Such a network, from now on denominated *thrust network*, is described by means of N_n nodes and N_b branches connecting pairs of nodes.

The thrust network is not used to geometrically model the volume occupied by the vaulted structure, as it happens, e.g., in finite element modelling; rather it is representative of the thrust forces that equilibrate the external loadings. Accordingly, branches of the network represent the direction of the thrust forces, similarly to the branches of a funicular polygon.

The n-th node of the network is characterized by its position (x_n, y_n, z_n), in a three-dimensional Cartesian reference frame in which z is the vertical direction. The generic branch b of the network is identified by two end nodes and the corresponding value of the thrust force, denoted as $\mathbf{t}^{(b)} = (t_x^{(b)}, t_y^{(b)}, t_z^{(b)})$.

Nodes are loaded both by an external force $\mathbf{f}^{(n)} = (f_x^{(n)}, f_y^{(n)}, f_z^{(n)})$, whose value depends on the region of influence of the node, and by the thrust forces pertaining to branches connected to the node; being compressive by assumption, these thrust forces are oriented towards node n. Branches can be labelled as *internal*, if they represent a thrust force that is interior to the network, *edge* if they represent forces that are on a free edge or *external* if they represent the

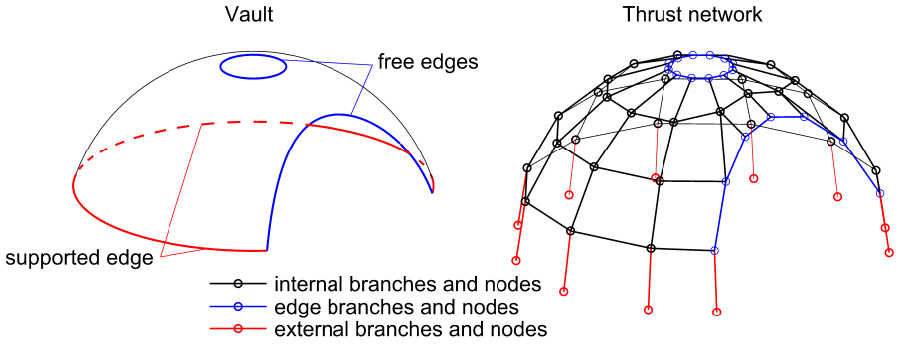

Figure 1: Restrained and free edges of a vault and their representation by external and edge branches and nodes

support reactions, see, e.g., Figure 1. Following the same logic, the set of nodes is split into N_i internal nodes, N_e edge nodes and N_r external (restrained) nodes, where only one external branch converges. Hence one has $N_n = N_i + N_e + N_r$.

While the horizontal position of internal and external nodes are assigned, the coordinates of the edge nodes are unknown. This is due to the fact that relevant edge branches, i.e. branches connected by edge nodes, will be funicular, in both the horizontal and vertical directions, of the internal thrusts and of the applied loads converging to edge nodes.

Equilibrium conditions are employed in order to evaluate branch thrusts, heights of internal and external nodes and the coordinates of boundary (edge) nodes. Such equations are written only for internal and edge nodes, while external nodes are used uniquely as endpoints of external branches that, in turn, represent support reactions. Accordingly, external nodes and branches are used to model the constraints of the vaulted structure.

2.1 Equilibrium of nodes

Following the approach illustrated in [9], the horizontal equilibrium of internal nodes is enforced by the $2N_i$ equations

$$\begin{cases} \mathbf{C}_i \hat{\mathbf{t}}_h + \mathbf{f}_{x,i}\, r = \mathbf{0}_i \\ \mathbf{S}_i \hat{\mathbf{t}}_h + \mathbf{f}_{y,i}\, r = \mathbf{0}_i \end{cases} \tag{1}$$

where $\mathbf{C}_i$ and $\mathbf{S}_i$ are coefficient matrices containing the cosine directors of the horizontal projections of the network branches; the subscript i indicates that only equilibrium of internal nodes is considered. The vector $\hat{\mathbf{t}}_h$ appearing in (1) collects branch reference thrusts $\hat{t}_h^{(b)} = r t_h^{(b)} = r\sqrt{t_x^{(b)2} + t_y^{(b)2}}$, while r is an unknown parameter and $\mathbf{0}_i$ is a vector of N_i zeros.

The coefficients $\mathbf{C}_i$ and $\mathbf{S}_i$ in (1) are obtained by selecting the rows relevant to the internal nodes from two coefficient matrices $\mathbf{C}$ and $\mathbf{S}$ that, in turn, contain the cosine directors of all branches of the network and are constructed by assembling branches' contributions for all N_i nodes of the network. In particular, the generic branch b, which connects nodes n and $m^{(b)}$, contributes to the b-th column of the matrices $\mathbf{C}$ and $\mathbf{S}$ by the terms

$$\mathbf{C}^{(b)} = \frac{1}{\ell_h^{(b)}} \begin{bmatrix} x_n - x_m^{(b)} \\ x_m^{(b)} - x_n \end{bmatrix} \qquad \mathbf{S}^{(b)} = \frac{1}{\ell_h^{(b)}} \begin{bmatrix} y_n - y_m^{(b)} \\ y_m^{(b)} - y_n \end{bmatrix} \tag{2}$$

that are assembled into rows n and $m^{(b)}$, being

$$\ell_h^{(b)} = \sqrt{\left(x_n - x_m^{(b)}\right)^2 + \left(y_n - y_m^{(b)}\right)^2} \tag{3}$$

Also the vertical equilibrium is enforced for all internal nodes of the network, so as to obtain a system of N_i linear equations that can be expressed in matrix form as

$$\mathbf{D}_i\mathbf{z} + \mathbf{f}_{z,i}\, r = \mathbf{0}_i \tag{4}$$

The entries of $\mathbf{D}_i$ are a combination of the reference thrust densities of the network branches and the subscript i is used to indicate that only the equilibrium of internal nodes is considered. The entries of $\mathbf{D}_i$ are computed by assembling the thrust densities of all branches. Specifically, for a generic branch b connecting nodes n and $m^{(b)}$ of the network, the coefficients

$$\mathbf{D}^{(b)} = \frac{\hat{t}_h^{(b)}}{\ell_h^{(b)}} \begin{bmatrix} 1 & -1 \\ -1 & 1 \end{bmatrix} \tag{5}$$

are evaluated and assembled in rows n and $m^{(b)}$ of columns n and $m^{(b)}$ of a coefficient matrix $\mathbf{D}$. Thus, the entries of the matrix $\mathbf{D}_i$, appearing in equations (4), are obtained by selecting the rows of $\mathbf{D}$ corresponding to internal nodes.

The vector $\mathbf{z}$ collects unknown heights of all nodes, while $\mathbf{f}_{z,i}$ is the vector of the vertical loads applied to the internal nodes.

The parameter r is used both in formulas (1) and (4) to select a solution corresponding to lower values of z (maximum thrust solution) or higher values of z (minimum thrust solution).

2.2 Solution procedure for networks subjected to horizontal and vertical loads

In presence of horizontal nodal forces equations (1) and (4) expressing in turn horizontal and vertical equilibrium of nodes are coupled by means of the unknown r so that their solution is more cumbersome to achieve. However if one sets a tentative value for r, say it $r^{(j)}$, the corresponding reference thrusts $\hat{\mathbf{t}}_h^{(j)}$ are evaluated by solving the linear optimization problem

$$\min_{\hat{\mathbf{t}}_h} \left(\mathbf{i}_b \cdot \hat{\mathbf{t}}_h^{(j)} \right) \text{ such that } \begin{cases} \begin{bmatrix} \mathbf{C}_i \\ \mathbf{S}_i \end{bmatrix} \hat{\mathbf{t}}_h^{(j)} = - \begin{bmatrix} \mathbf{f}_{x,i}\, r^{(j)} \\ \mathbf{f}_{y,i}\, r^{(j)} \end{bmatrix} \\ \hat{\mathbf{t}}_h^{(j)} \geq \hat{\mathbf{t}}_{h,\min} \end{cases} \tag{6}$$

obtained from the horizontal equilibrium equations (1). In formula (6) $\mathbf{i}_b = (1, 1, ..., 1)$ has N_b entries so that the product $\mathbf{i}_b \cdot \hat{\mathbf{t}}_h^{(j)}$ represents the sum of all components of $\hat{\mathbf{t}}_h^{(j)}$. This particular choice for the objective function is useful to obtain a solution $\hat{\mathbf{t}}_h^{(j)}$ that is as close as possible to the assigned minimum values $\hat{\mathbf{t}}_{h,\min}$.

The reference thrusts $\hat{\mathbf{t}}_h^{(j)}$ obtained from the solution of (6) can be used to evaluate the x and y coordinates of the edge nodes by means of the equations

$$\begin{aligned} \mathbf{x}_{i+e}^{(j)} &= - \left[\mathbf{D}_{i+e\,i+e}^{(j)} \right]^{-1} \left[\mathbf{D}_{i+e\,r}^{(j)} \mathbf{x}_r + \mathbf{f}_{x,i+e}\, r^{(j)} \right] \\ \mathbf{y}_{i+e}^{(j)} &= - \left[\mathbf{D}_{i+e\,i+e}^{(j)} \right]^{-1} \left[\mathbf{D}_{i+e\,r}^{(j)} \mathbf{y}_r + \mathbf{f}_{y,i+e}\, r^{(j)} \right] \end{aligned} \tag{7}$$

Depending on the geometry and connectivity of the network, the procedure described above modifies the positions of internal and edge nodes. In general this effect is negligible for internal nodes but, should their position be significantly modified by the application of formula (7), external loads need to be recomputed.

Once the j-th estimate of the horizontal position of all nodes is assigned, nodal heights and a new $(j+1)$ estimate of r are evaluated from (4) by solving the linear optimization problem

$$\min_{\mathbf{z},r} \pm r^{(j+1)} \text{ such that } \begin{cases} \left[\mathbf{D}_i^{(j)} \; \mathbf{f}_{z,i}\right] \begin{bmatrix} \mathbf{z}^{(j)} \\ r^{(j+1)} \end{bmatrix} = \mathbf{0}_i \\ \begin{bmatrix} \mathbf{z}_{\min} \\ 0 \end{bmatrix} \leq \begin{bmatrix} \mathbf{z}^{(j)} \\ r^{(j+1)} \end{bmatrix} \leq \begin{bmatrix} \mathbf{z}_{\max} \\ +\infty \end{bmatrix} \end{cases} \tag{8}$$

where $\mathbf{z}_{\min}$ and $\mathbf{z}_{\max}$ are the lower- and upper-bounds imposed by the designer to the nodal heights of the network. Usually, for internal nodes they can be set equal to the heights of the intrados and extrados of the vault; alternatively, to reach a full compression of the vault section, they can be set equal to the heights corresponding to the lower and upper third of the vault thickness.

The objective function $\pm r$ is set equal to $+r$ if one looks for a solution that minimizes r, thus obtaining the shallowest configuration of the network. Conversely, one sets $-r$ to obtain a solution that maximizes r, what is relevant to the deepest network. In both cases, positive values of r are estimated since the constraint $0 \leq r \leq +\infty$ is imposed in (8).

If the difference between two successive estimates of r is lower than a given tolerance, i.e.

$$\left| \frac{r^{(j+1)} - r^{(j)}}{r^{(j)}} \right| < tol \tag{9}$$

the procedure is terminated. If the previous condition is not fulfilled, the procedure is reiterated by solving (6), (7) and (8), and verifying again the fulfilment of (9).

Once solution is reached, actual branch's thrusts are evaluated by composing the horizontal and vertical reference thrusts of each branch, according to

$$t^{(b)} = \sqrt{\left[t_h^{(b)}\right]^2 + \left[t_z^{(b)}\right]^2} = \frac{\hat{t}_h^{(b)}}{r} \frac{\ell^{(b)}}{\ell_h^{(b)}} \tag{10}$$

where $\ell^{(b)}$ is the length of the b-th branch.

2.3 An optimized iterative solution procedure in absence of edge nodes

In case the network is lacking of edge nodes, an optimized procedure can be employed. Actually, since the conditions in (6) are linear, the generic solution $\hat{\mathbf{t}}_h^{(j)}$, corresponding to a given value of $r^{(j)}$, can be expressed as

$$\hat{\mathbf{t}}_h^{(j)} = \hat{\mathbf{t}}_h^{(0)} + \frac{r^{(j)}}{r^{(1)}} \left[\hat{\mathbf{t}}_h^{(1)} - \hat{\mathbf{t}}_h^{(0)}\right] \quad \text{if} \quad r^{(j)} \geq r^{(1)} \tag{11}$$

where $\hat{\mathbf{t}}_h^{(0)}$ and $\hat{\mathbf{t}}_h^{(1)}$ are the reference thrusts returned by the linear optimization (6) in which it has been set $r = r^{(0)} = 0$ and $r = r^{(1)} = r_1$, r_1 being an arbitrary positive scalar.

It is straightforward to verify that (11) fulfils both the equality and the inequality conditions on the right-hand side of (6), provided that $r^{(j)} > r_1$; hence thrusts associated with $r^{(j)}$ can be assumed as a solution that fulfils horizontal equilibrium of nodes and the linear optimization problem (6) can be solved only twice.

Once $\hat{\mathbf{t}}_h^{(0)}$ and $\hat{\mathbf{t}}_h^{(1)}$ have been evaluated, the reference thrusts $\hat{\mathbf{t}}_h^{(1)}$ are used in (8) to obtain the nodal heights and the tentative value $r^{(j+1)}$. This estimate of r is used in (11) to obtain a new value of reference thrusts that, in turn, is used again in (8) to obtain a new estimate of r. The procedure is iterated until the convergence condition (9) is fulfilled. Finally, at convergence, formula (10) is applied to evaluate actual values of thrust in each branch of the network.

3 Numerical examples

Four numerical examples are reported below. The first two of them concern the analysis of a three centred arch while the last two address the full three-dimensional analysis of two spherical domes that only differ for the presence of a circular opening at the top. For all examples we show two solutions, corresponding to the deepest and shallowest configurations of the network, respectively. Indicating by r_d the value of r associated with the deepest configuration of the network and by r_s the one associated with the shallowest configuration, we will show that the ratio r_s/r_d is related to the safety factor of the arch or vault and it can be used to characterize a limit condition for the structure.

3.1 Minimum thickness of a three-centred arch

We consider the three-centred arch of Figure 2 having centres $C_1 \equiv (-2m, 0m)$, $C_2 = (0m, -4m)$, $C_3 = (2m, 0m)$, radii $R_2 = 6m$, $R_1 = R_3 = R_2 - \sqrt{2^2+4^2} \approx 1.53m$ and springing angles $\alpha = \beta = \pi/10$. The arch has thickness $t = 0.4m$ and is subjected only to self-weight, this is evaluated by considering a weight per unit area equal to $\rho = 8kN/m^2$. The corresponding deepest and shallowest configurations of the thrust network are reported in Figure 3.

Thus is clear how the two network configurations are visibly different. This is confirmed by the value of the ratio $r_s/r_d = 1.6585$ that, being different from unity, emphasizes that forces within the arch have the possibility to adapt to changes in the loading condition or to settlements of the structure.

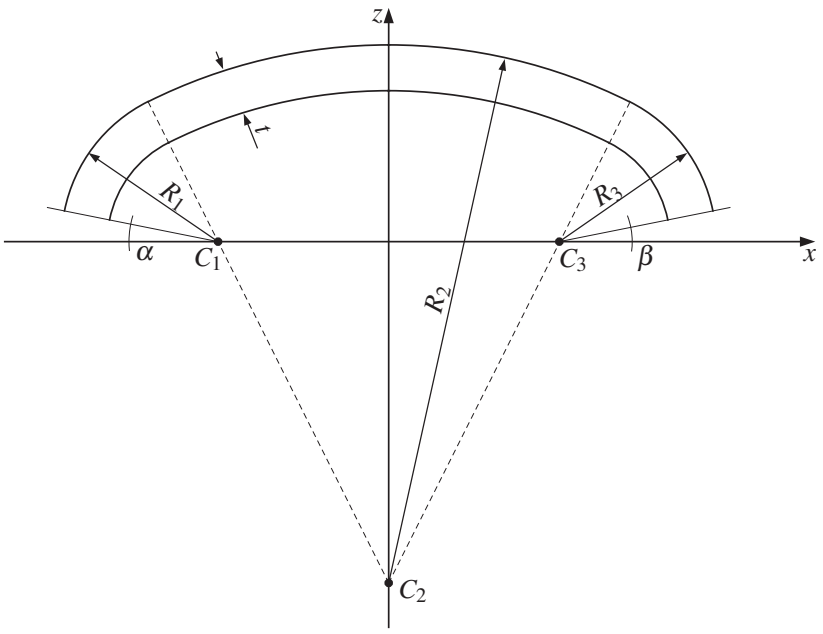

Figure 2: Three-centred arch

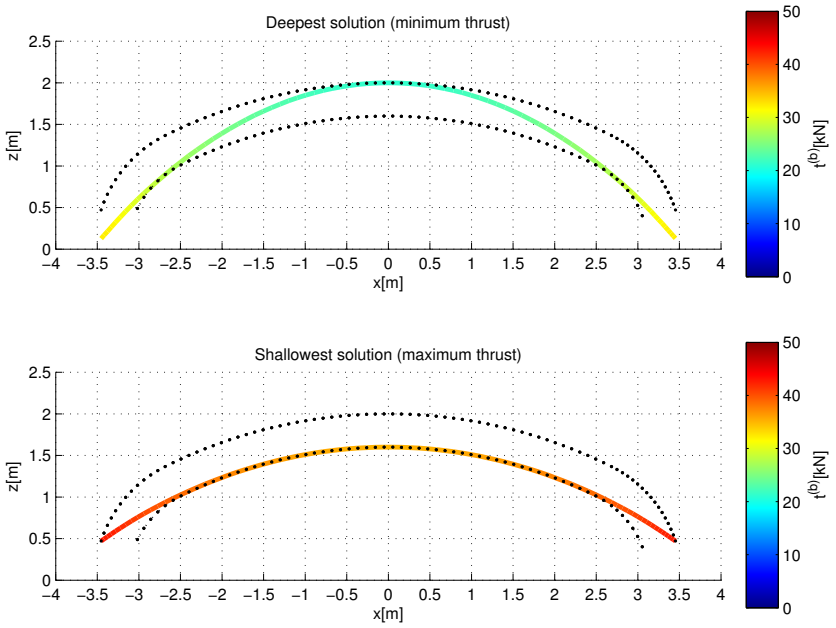

Figure 3: Three-centred arch: deepest and shallowest network configurations for the arch of thickness $t = 0.4\,m$ subjected to self weight

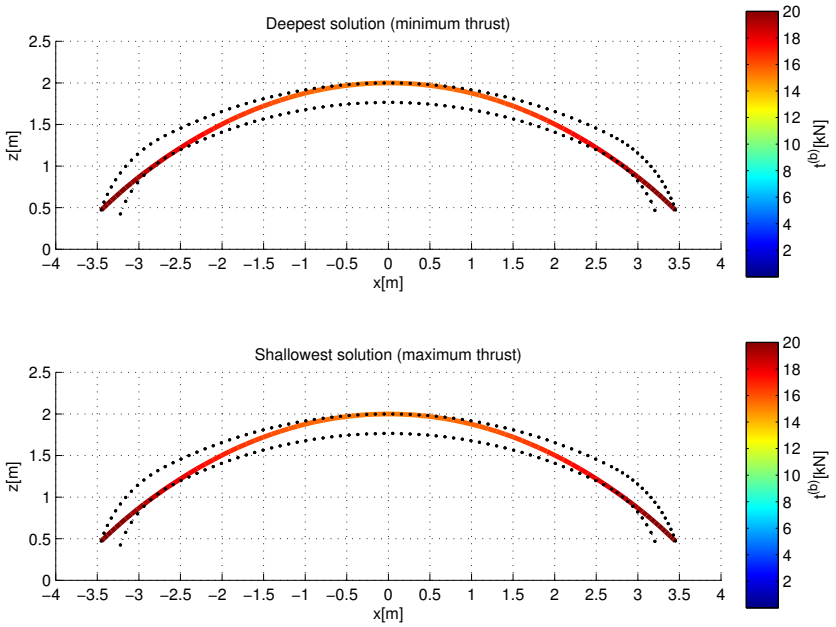

Figure 4: Three-centred arch: coincidence of the deepest and shallowest network configurations for the arch subjected to self weight emphasizes that the minimum thickness ($t = 0.234\,m$) has been attained

A second analysis has been carried out by progressively reducing the thickness of the arch to the value $t = 0.234\,m$, what corresponds to a unit value of the ratio r_s/r_d. Indeed, as shown in Figure 4, the deepest and shallowest configurations of the network are indistinguishable, so that the minimum limit value of the arch thickness has been reached.

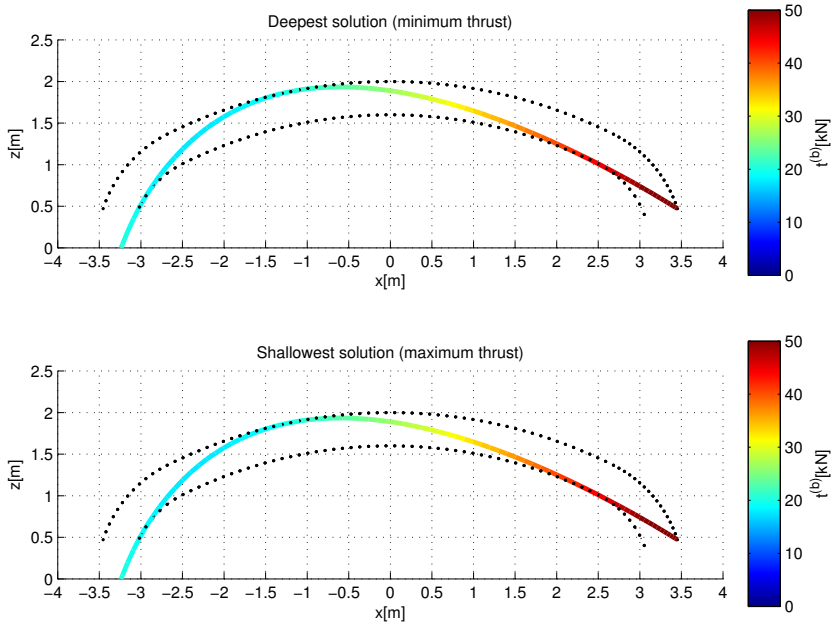

Figure 5: Three-centred arch: deepest and shallowest network configurations for the arch having thickness $t = 0.4m$ subjected to vertical and horizontal loads applied according to the ratio $f_h/f_z = 0.821$

3.2 Maximum horizontal load of a three-centred arch

The same approach used for determining the minimum arch thickness can be exploited to evaluate the horizontal load bearing capacity of the arch. The arch under consideration is the same described earlier and has thickness $t = 0.4m$. Horizontal forces are kept proportional to the vertical ones so that the analysis has been carried out by progressively increasing the value of the ratio f_h/f_z until the deepest and shallowest configuration of the network become coincident as in Figure 5. Such a condition is characterized by $r_s/r_d = 1$ and, in this case, it is attained when the ratio between the horizontal and vertical loads reaches the limit value $f_h/f_z = 0.821$.

3.3 Maximum horizontal load of a hemispherical dome

In order to show how this approach can be applied also to three-dimensional networks, we consider a hemispherical dome of diameter $D = 4m$ and thickness $t = 0.2m$. Branches of the network are directed along the meridians and parallels of the dome, converging to a node placed at the top.

Both vertical and horizontal forces are applied at the nodes of the network proportionally to the self-weight of the dome. In particular, vertical forces applied at the top node is $f_z = 6kN$, nodes of the first parallel, i.e. the one closer to the top node, is $f_z = 4kN$, while the forces $f_z = 6kN$, $f_z = 8kN$ and $f_z = 12kN$ are applied at the nodes of the second, third and fourth parallel, respectively. Horizontal forces act along the x axis and are kept proportional to the vertical ones.

The ratio r_s/r_d attains the value 1.4029 if horizontal forces are ignored, confirming the visible difference between the deepest and shallowest configuration of the thrust network, see, e.g. Figure 6.

The analysis of the dome subjected to the combined action of vertical and horizontal loads has been carried out by progressively increasing the value of the ratio f_h/f_z till the attainment of the limit condition $r_s/r_d = 1$. As shown in Figure 7, an intermediate solution, corresponding

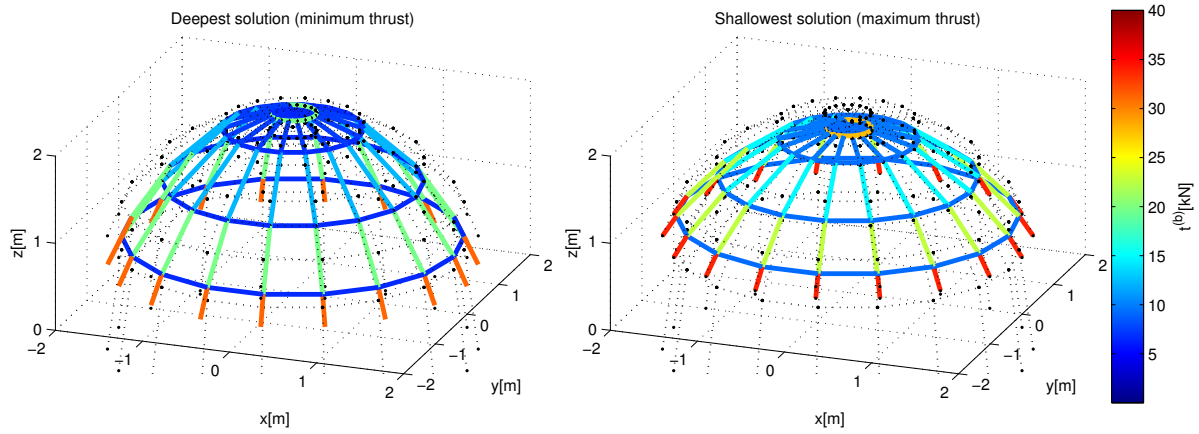

Figure 6: Hemispherical dome: deepest and shallowest network configurations for dome subjected to self-weight

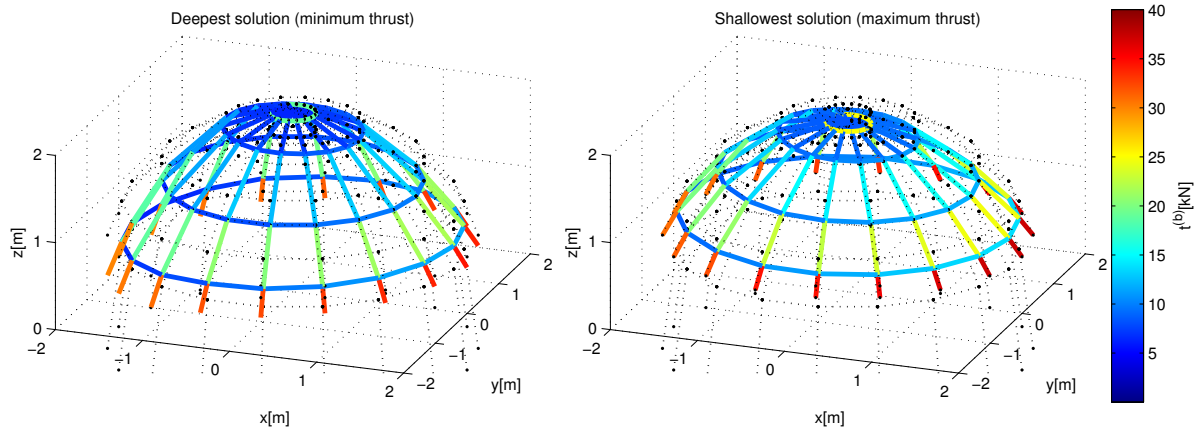

Figure 7: Hemispherical dome: deepest and shallowest network configurations for dome subjected to self-weight and horizontal loads applied according to the ratio $f_h/f_z = 0.08$

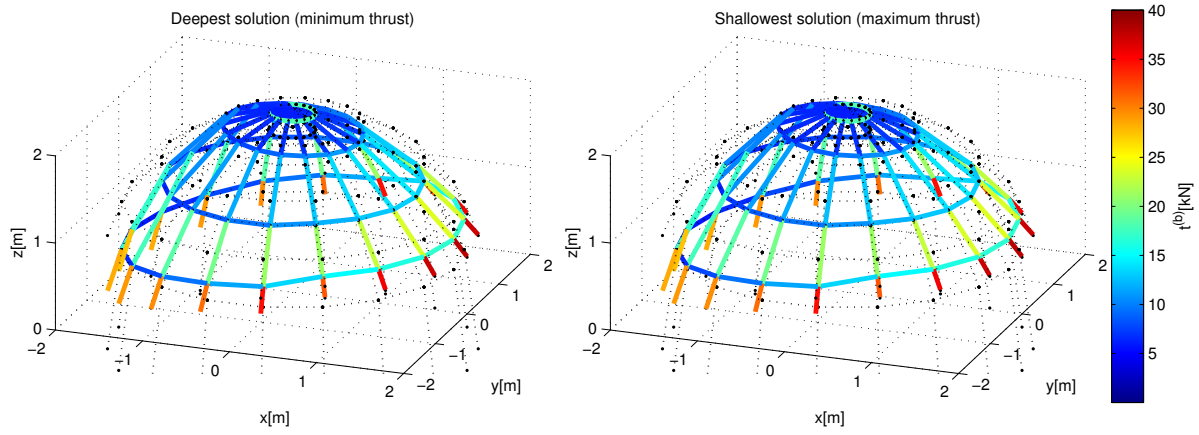

Figure 8: Hemispherical dome: deepest and shallowest network configurations for dome subjected to self-weight and horizontal loads applied according to the ratio $f_h/f_z = 0.159$

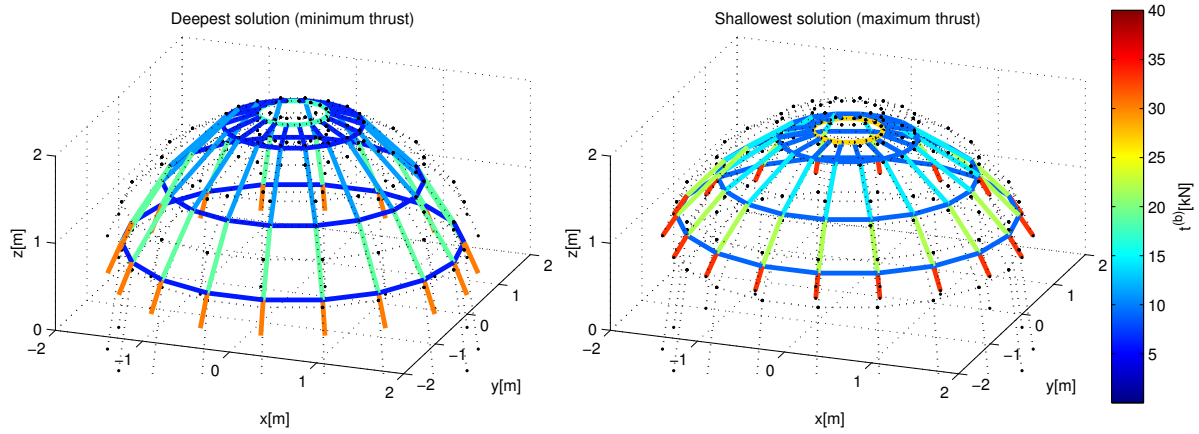

Figure 9: Dome with oculus: deepest and shallowest network configurations for dome subjected to self-weight

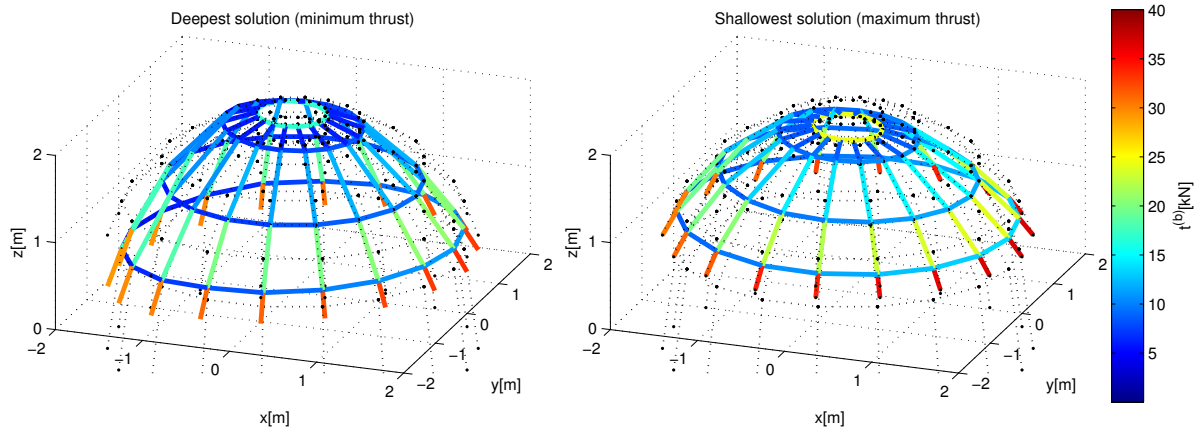

Figure 10: Dome with oculus: deepest and shallowest network configurations for dome subjected to self-weight and horizontal loads applied according to the ratio $f_h/f_z = 0.08$

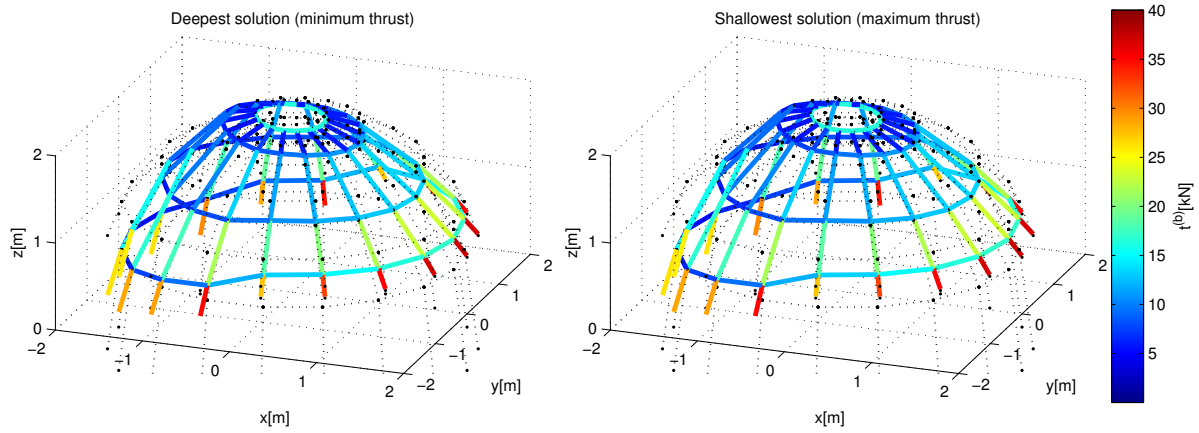

Figure 11: Dome with oculus: deepest and shallowest network configurations for dome subjected to self-weight and horizontal loads applied according to the ratio $f_h/f_z = 0.171$

to $f_h/f_z = 0.08$, still exhibits a visible difference between the deepest and shallowest configurations of the thrust network, confirmed by the value attained by the ratio $r_s/r_d = 1.3215$.

Finally, the limit value of the horizontal forces, corresponding to $r_s/r_d = 1$, is attained when $f_h/f_z = 0.159$; in this case the deepest and the shallowest configurations of the network, reported in Figure 8, become indistinguishable.

3.4 Maximum horizontal load of a hemispherical dome with oculus

As a final example we consider the dome analysed in the previous subsection in which a circular opening (oculus) of diameter $d = 0.8\,m$ is present at the top. The corresponding network is obtained from the one used for the previous example by deleting the top node and all branches converging to it. Also loadings are equal to the ones considered in the previous example, except for the force applied to the top node.

Thrust network configurations corresponding to the network subjected to self-weight is reported in Figure 9, in which the difference between the deepest and shallowest configurations of the thrust network is quantified by the ratio $r_s/r_d = 1.5195$. Such a ratio reduces as the horizontal forces are applied. In particular, for a value of horizontal forces corresponding to the ratio $f_h/f_z = 0.08$, the deepest and shallowest configurations of the network, plotted in Figure 10, are still sensibly different; this is witnessed by the value of the ratio $r_s/r_d = 1.4355$. Conversely, when the limit value of horizontal loads is attained, i.e. when $f_h/f_z = 0.171$, the deepest and shallowest configuration of the network are coincident, see, e.g., Figure 11, and the ratio r_s/r_d attains a unit value.

By comparing Figure 8 and Figure 11, and the corresponding limit values of the ratio f_h/f_z, associated with a ratio $r_s/r_d = 1$, that amount respectively to 0.171 and 0.159, one infers that the seismic safety of the dome with oculus is greater than the one pertaining to the hemispherical dome.

REFERENCES

[1] M. Angelillo, L. Cardamone, A. Fortunato, A numerical model for masonry - like structures. *Journal of Mechanics of Materials and Structures*, **5**:415-583, 2010.

[2] P. Block, *Thrust Network Analysis*. PhD thesis, Massachusetts Institute of Technology, 2009.

[3] P. Block, L. Lachauer, Three-dimensional equilibrium analysis of gothic masonry vaults. *International Journal of Architectural Heritage*, **8**:1-24, 2014.

[4] F. Fraternali, A thrust network approach for the equilibrium problem of unreinforced masonry vaults via polyhedral stress functions. *Mechanics Research Communications*, **37**:198-204, 2010.

[5] J. Heyman, *The masonry arch*. Ellis Horwood, Chichester, 1982.

[6] J. Heyman, *The Stone Skeleton: Structural Engineering of Masonry Architecture*. Cambridge University Press, Cambridge, 1995.

[7] S. Huerta, The analysis of masonry architecture: a historical approach. *Architectural Science Review*, **51**:297-328, 2008.

[8] R. Hooke, *A description of helioscopes and some other instruments*. T.R. for John Martyn, London, 1676.

[9] F. Marmo, L. Rosati, Reformulation and extension of the thrust network analysis. *Computers and Structures*, **182**:104-118, 2017.

[10] D. O'Dwyer, Funicular analysis of masonry vaults. *Computers and Structures*, **73**:187-197, 1999.

[11] A. Tralli, C. Alessandri, G. Milani, G. (2014) Computational methods for masonry vaults: a review of recent results. *The Open Civil Engineering Journal*, **8**:272-87, 2014.